ELEVENTH INTERNATIONAL CONFERENCE ON INTERGRANULAR AND INTERPHASE BOUNDARIES 2004

JOURNAL OF MATERIALS SCIENCE **40** (2005) 3243–3246

The role of vicinal Σ3 boundaries and Σ9 boundaries in grain boundary engineering

V. RANDLE*, YAN HU
Materials Research Centre, School of Engineering, University of Wales Swansea, Swansea SA2 8PP, UK
E-mail: v.randle@swansea.ac.uk

Σ3 grain boundary planes and triple junctions containing Σ3 boundaries have been investigated in grain boundary engineered brass using an adaptation of electron backscatter diffraction (EBSD) data combined with a single surface trace analysis methodology. The data have been analysed from the standpoint of whether or not the interface planes in the Σ3 boundaries are close to {111} (i.e. coherent annealing twins), vicinal to {111} (i.e. a small deviation from the {111} reference structure) or not on {111}. At triple junctions composed of Σ3/Σ3/Σ9 it was shown that a combination of one {111} and one vicinal-to-{111} Σ3 was more likely to occur than two {111} Σ3s or two not-{111} Σ3s. The explanation for the preferred {111}/vicinal-to-{111} combination is that mobile Σ9 boundaries with high deviations encounter {111} Σ3s, and in consequence regenerate a Σ3 at the triple junction which must be vicinal-to-{111} according to the crystallographic constraints at the junction. Analysis of the not-{111} Σ3s indicated that more than half the boundaries in this category could not have {211}{211}, {774}{855}, {111}{511}, {001}{221} or {110}{411} planes. The possible distribution of these planes types, based on information from the single-surface trace analysis, had a high rank correlation coefficient, 0.925, with previous data from nickel which was based on a two-surface, full boundary planes analysis.

1. Introduction

Grain boundary engineering is the deliberate manipulation of grain boundary structure in order to improve material properties such as corrosion resistance, intergranular cracking or ductility. Interfaces classified as Σ3 in coincidence site lattice notation are of technological relevance to GBE, and the term GBE is most usually applied to the exploitation of prolific annealing twinning in order to bring about the desired property improvements. Σ3s can either be coherent twins (i.e. on {111}), or have other rational or irrational boundary planes. The properties of each group are different. Furthermore it has been found that there are groups of Σ3s which are 'vicinal' to {111}, i.e. a small deviation from the {111} reference structure is accommodated by steps on the boundary plane [1]. Several investigations have consistently shown that many Σ3 boundaries are in fact either vicinal to the coherent twin reference structure or vicinal to another reference structure such as an asymmetrical tilt configuration [e.g. 2].

The different behaviours of the various types of Σ3 boundaries complicates interpretation of data, particularly if misorientation only is measured. Grain boundary misorientation measurements are acquired by automated electron backscatter diffraction (EBSD) in an SEM [3]. The principal disadvantage is that only part of the grain boundary crystallography, the misorientation and not the interface plane, is measured automatically. Moreover the standard EBSD data processing algorithms classify all Σ3 boundaries together. There is a need for a rigorous and efficient method to categorise the different Σ3 types as an extension to standard EBSD in order to characterise and to understand these interfaces further. This objective has particular application to grain boundary engineering. Furthermore, characterisation of triple junctions which contain Σ3 boundaries is relevant to grain boundary engineering, because these ultimately control the constitution of the interfacial network which in turn controls interface properties.

Several workers are now directing research initiatives towards extracting more in-depth information from orientation mapping investigations of the grain boundary network. One strand is to measure the grain boundary plane crystallography. Recently the method for determination of boundary planes has been refined for certain well-defined crystallographies by the use of a single-surface trace analysis procedure, which has the advantage of greatly reducing the large experimental effort and eliminating the serial sectioning errors involved in boundary plane determination [4, 5]. This new method has been used to identify Σ3 boundary

*Author to whom all correspondence should be addressed.

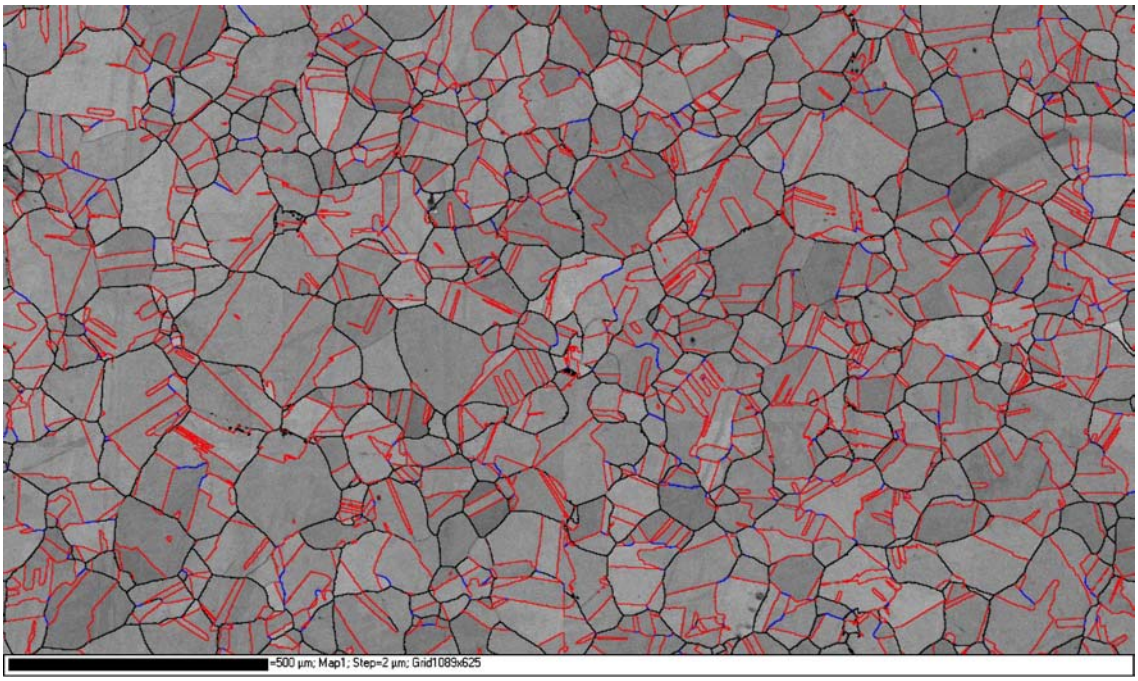

Figure 1 Example of an orientation map from grain boundary engineered brass. High angle boundaries, Σ3 boundaries and Σ9 boundaries are black, red and blue respectively.

facets which are not {111}, those boundaries which are probably {111}, and those which are probably vicinal to {111} [5, 6].

This paper reports recent experimental work on grain boundary engineered brass, with regard to the interface plane types of Σ3s and the constitution of triple junctions which contain Σ3s.

2. Experimental

Specimens of alpha-brass were strained 25% by uniaxial tension, followed by an anneal in air for 300 s at 665°C. This procedure was carried out five times in total in order to produce a grain boundary engineered microstructure. Specimens were prepared by normal metallographic procedures, plus a final polish in silica slurry to give a suitable surface finish for EBSD.

Misorientation data across interfaces were obtained by use of an EBSD system from HKL Technology (CHANNEL5) in a Philips XL30 scanning electron microscope (SEM) operated at 20 kV accelerating voltage. Several orientation maps with a grid step size of 2 μm were collected from each specimen, to give a total of over 21,000 grains. Approximately 500 Σ3s were selected for single-surface trace analysis of the boundary planes, which was carried out using dedicated programmes written in-house in visual BASIC. The single-surface trace analysis used here is described in detail elsewhere [5, 6].

3. Results and discussion

3.1. Microstructure and Σ3 boundary plane types

The total proportion of Σ3s and Σ9s in the microstructure was 54.4% and 3.5% respectively, calculated as a fraction of total boundary length. The typical microstructure is shown on an orientation map in Fig. 1. High angle boundaries, Σ3 boundaries and Σ9 boundaries are black, red and blue respectively.

A subset of Σ3s was selected for single-surface trace analysis to determine the crystallographic vector in the boundary plane, T. In the analysis each measured, in-plane vector T was tested to see if the Σ3 plane normal could be <111>. The critical experimental parameters are t_A and t_B, the complement of the angle between T and <111> in any two neighbouring grains A and B respectively. For an exact {111} coherent twin, $t_A = t_B = 0°$. Three groups were identified:

1. 'Not-{111}': Σ3s where the average value of t_A and t_B was >10°: boundary definitely not {111}.
2. '{111}': Σ3s where the average of t_A and t_B was <2° and the deviation from the reference misorientation was <2°: boundary very likely to be on {111} and classified as the exact coherent twin reference structure.
3. 'Vicinal-to-{111}': Σ3s where the average of t_A and t_B was 2°–10° and the deviation from the reference misorientation was <2°: boundary very likely to be vicinal to the {111} reference structure.

The sample population is biased since Σ3 interfaces which were assumed on the basis of their morphology (e.g. pairs of twins) to be probably {111} were omitted from the sampling for economy of effort. The not-{111} group, which were proved to be not on {111} or vicinal to it, comprised more than one-third of the sample population. This is a significant result since in many investigations the whole Σ3 category is tacitly assumed, from misorientation data alone, to be on {111} and therefore to have very low energy. In the not-{111} group here it could not be forecast from morphology that such interfaces were not {111} or vicinal-to-{111}. Furthermore within the group that has been called not-{111}

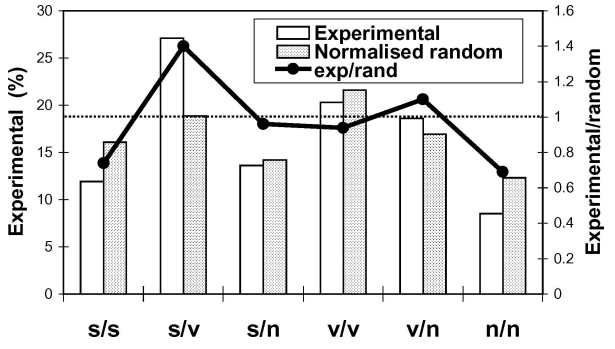

Figure 2 Average proportions of combinations of Σ3 types at triple junctions which are composed of Σ3/Σ3/Σ9, by experimental observation and calculation of the proportions expected in a random distribution. The ratio of experimental-to-random is marked as a line. s: {111}; v: vicinal-to-{111}; n: not-{111}.

here, some interfaces may in fact be vicinal to reference structures other than {111}. These are reported and discussed below.

There are nearly as many vicinal-to-{111} Σ3s in the sample population as there are not-{111} Σ3s. These vicinal-to-{111} boundaries cannot be recognised by the angular deviation from the reference misorientation. For the combined group comprising {111} and vicinal-to-{111} boundaries (which were both classified as having misorientation deviation $<2^\circ$) the average deviation was $<1^\circ$. The average misorientation deviation for the not-{111} group was higher than the combined {111} and vicinal-to-{111} group, nearly 2°. Hence there is a distinction, albeit small, between not-{111} Σ3s and those related to {111} on the basis of average misorientation deviation. For the {111} and vicinal-to-{111} groups it is important that *both* t_A and t_B conform to the categorisation criterion in the data analysis, since the interface plane is {111} or near {111} (within 10°) in *both* grains for the {111} and vicinal-to-{111} structure respectively.

Since nearly half of the interface length in the specimens is Σ3, a significant proportion of triple junctions include two Σ3s. The third boundary in such triple junctions is a Σ9, providing that the misorientation of the Σ3s is sufficiently close to the reference misorientation. In the present data sets, the Σ9 segments tend to be short 'bridges' between Σ3s.

Six different combinations of {111}, vicinal-to-{111} or not-{111} Σ3s can occur at triple junctions which comprise Σ3/Σ3/Σ9: {111}/{111}, {111}/vicinal-to-{111}, {111}/not-{111}, vicinal-to-{111}/vicinal-to-{111}, vicinal-to-{111}/not-{111} and not-{111}/not-{111}. The measured proportion of each combination is shown on Fig. 2. Fig. 2 also includes the proportions of each combination that would be expected based on statistical distribution alone, normalised by the proportion of each Σ3 type in the sample population. Finally on Fig. 2 the proportions of experimentally measured combinations relative to the theoretical combinations are shown. For the {111}/not-{111}, vicinal-to-{111}/vicinal-to-{111} and vicinal-to-{111}/not-{111} combinations the measured proportions were close to those based on statistical combinations. On the other hand there were more {111}/vicinal-to-{111} combinations and less {111}/{111} and not-{111}/not-{111} combinations in the triple junction population.

Fig. 2 shows that the most frequently observed Σ3 combination at a triple junction is a {111} and a vicinal-to-{111} Σ3. This combination occurred more frequently than two {111} Σ3s or two not-{111} Σ3s. An explanation for this distribution reflects how the Σ3s originated. Newly generated annealing twins are {111}. As more annealing twins were generated, mutual impingements occurred whereby two Σ3s generated a Σ9. The Σ9 is a mobile boundary and therefore it can migrate under an appropriate driving force, acquiring a deviation from the reference misorientation and plane as it does so. When, during migration, the Σ9 encountered a Σ3 (probably {111}, because of the high incidence of annealing twinning) a new Σ3 was regenerated according to the 'Σ3 regeneration model' [7]. The model relies on the condition that an encounter between a Σ9 and a Σ3 gives a Σ3 boundary rather than a Σ27. This is supported by experimental evidence since relatively few Σ27 boundaries are reported in investigations even when the proportion of Σ3s is very high [e.g. 8]. Furthermore, the generation of an incoherent Σ3 rather than a Σ27 is generally preferred both on the basis of lower energy and greater mobility. By the same argument if a Σ9 does encounter a Σ27, a Σ3 would again be generated rather than a Σ243. In general, then, it can be stated

$$\Sigma 3^n + \Sigma 3^{n+1} \rightarrow \Sigma 3 \qquad (1)$$

rather than the following reaction to produce higher $\Sigma 3^n$ variants:

$$\Sigma 3^n + \Sigma 3^{n+1} \rightarrow \Sigma 3^{n+2} \qquad (2)$$

The reaction in Equation 1 is a method by which *mobile* Σ3s—which still have markedly different properties to random boundaries even though they are not the {111} type—enter the microstructure. Once additional Σ3s have been generated by this means, it has been shown that further annealing can allow grain boundary planes to approach more closely low volume configurations if grain growth is minimised [9].

In the present data because the Σ9 misorientation and plane were displaced from the reference value, the new, regenerated Σ3 must also be displaced from the reference structure, in order to preserve the crystallography at the triple junction. This mechanism accounts for the higher than random proportion of {111}/vicinal-to-{111} Σ3s observed at triple junctions, and conversely the low proportion of {111}/{111}.

4. Incoherent Σ3 planes

The boundaries that have been categorised as not-{111}may not necessarily have irrational boundary planes. Σ3 plane combinations also include the symmetrical {211} 'incoherent twin', and various asymmetrical tilt boundaries and twist boundaries. Both calculation and experimental measurements on bicrystal specimens have shown that Σ3 <110> tilt boundaries

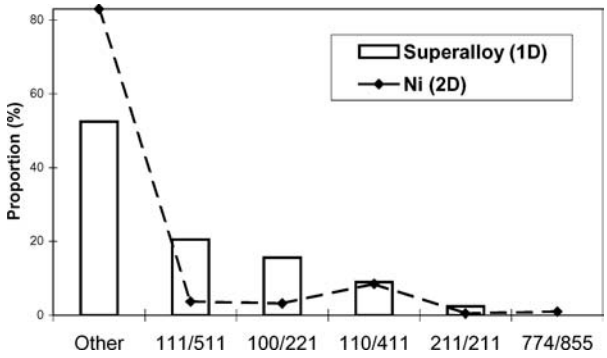

Figure 3 Further analysis of the population of Σ3s categorised as not-{111}. Various tilt boundary plane combinations are labelled, plus a category labelled 'other' which comprises the remaining data in the population which is not one of the tilt combinations labelled. Data from a previous investigation on nickel [7] is included as a dashed line.

in copper lie in an energy valley [10]. Moreover, the four strongest reflections from the 'sphere-on-plate' experiments in copper and silver, were {111}{111}, {110}{411} {100}{221} ('very strong') and {111}{511} ('strong'), which are all Σ3 <110> tilts [11]. The importance of one low-index plane at an interface has also been emphasised elsewhere [12].

The methodology used here to test for {111} was modified to enable testing for a number of other plane combinations. The plane combinations selected were the symmetrical tilt {211} and four asymmetrical tilts on <110>, namely {111}{511}, {100}{221}, {110}{411}, and {774}{855}. These particular asymmetrical tilts were selected because the first three include one low index plane, and conversely {774}{855} is an example of a Σ3 <110> asymmetric tilt which does not have a low-index plane.

Fig. 3 shows the results of the single-surface trace analysis for {211} symmetrical tilt and the four asymmetrical tilts in that portion of the Σ3 population which had been categorised as not-{111}. An interface was classified as possibly being one of the selected plane types if both t_A and t_B were $<2^\circ$, where the {111} reference plane was replaced by those planes listed above and shown on Fig. 3. It was found that just over half the interfaces could not be any of the plane combinations tested. Of the remaining cases, possible asymmetrical tilts having one low-index plane ({111}{511}, {100}{221} and {110}{411}) were all significantly represented whereas a possible {112} symmetrical tilt had hardly any representation and a possible {774}{855} none at all. It should be emphasised that these data describe either the proportion of interfaces which could *definitely* not be any of the planes tested (labelled 'other' on Fig. 3) or the proportions of interfaces that *might* be one of the plane combinations tested.

The present data, which show potential proximity to other Σ3 tilt boundaries on <011>, is supplemented on Fig. 3 by previously published data on distributions of Σ3s in nickel where all five degrees of freedom have been measured [13]. Fig. 3 shows that for both the previous nickel specimens and the present brass specimen only low proportions of {211}{211} and {774}{855} are present (or possible, in the present case where only the boundary trace has been measured). These proportions are less than in the group having one low index plane, namely {111}{511}, {001}{221} or {110}{411}. For both the nickel and the superalloy most of the not-{111} boundaries are in the 'other' category. There is a high rank correlation coefficient of 0.925, calculated from all the data shown in Fig. 3, between the new (single-surface) trace analysis reported here and the previous (two-surface) measurements on nickel. This high correlation coefficient gives confidence that the single-surface sectioning method has potential value for determining the probability of plane types other than {111}, especially given its experimental accuracy and simplicity compared to determination of all five degrees of freedom. More work is underway on this topic.

5. Conclusions

1. At triple junctions composed of Σ3/Σ3/Σ9 it was shown that a combination of one {111} and one vicinal-to-{111} Σ3 was more likely to occur than two {111} Σ3s or two not-{111} Σ3s. The explanation for the preferred {111}/vicinal-to-{111} combination is that mobile Σ9 boundaries with high deviations encounter {111} Σ3s, and in consequence regenerate a Σ3 at the triple junction which must be vicinal-to-{111} according to the crystallographic constraints at the junction.

2. Analysis of the not-{111} Σ3s indicated that more than half the boundaries in this category could not have {211}{211}, {774}{855}, {111}{511}, {001}{221} or {110}{411} planes. The possible distribution of these planes types, based on information from the single-surface trace analysis, had a high rank correlation coefficient, 0.925, with previous data from nickel which was based on a two-surface, full boundary planes analysis.

References

1. D. WOLF, in "Materials Interfaces: Atomic Level Structure and Properties", edited by D Wolf and S. Yip (Chapman & Hall, London, 1992) p. 1.
2. V. RANDLE and P. DAVIES, *Interf. Sci.* **7** (1999) 5.
3. V. RANDLE, in "Microtexture Determination and its Applications", 2nd edn (Institute of Materials, London, 2003).
4. S. I. WRIGHT and R. J. LARSEN, *J. Microsc.* **205** (2002) 245.
5. V. RANDLE and H. DAVIES, *Ultramicrosc.* **90** (2002) 153.
6. H. DAVIES and V. RANDLE, *J. Microsc.* **205** (2002) 253 .
7. V. RANDLE, *Acta. Mater.* **47** (1999) 4187.
8. V. RANDLE, in "The Role of the Coincidence Site Lattice in Grain Boundary Engineering" (Institute of Materials, London, 1996).
9. V. RANDLE, P. DAVIES and B. HULM, *Philos. Mag. A* **79** (1999) 305.
10. U. WOLF, F. ERNST, T. MUSCHIK, M. W. FINNIS and H. F. FISCHMEISTER, *Philos. Mag. A* **66** (1992) 991.
11. R. W. BALLUFFI and R. MAURER, *Scripta Metall.* **22** (1988) 709.
12. D. WOLF and J. F. LUTSKO, *Zeit. Kristall.* **189** (1989) 239.
13. V. RANDLE, *Acta. Mater.* **46** (1997) 1459.

Received 18 October 2004
and accepted 31 January 2005